atmosphere

MDPI

Article

Impacts of Biomass Burning, Urbanization, and Regional Environmental Conditions on Air Quality in Medium-Sized Cities in Brazil

Paula Florencio Ramires [1,2,*], Washington Luiz Félix Correia Filho [2], Rodrigo de Lima Brum [3] and Flavio Manoel Rodrigues da Silva Júnior [2,3]

[1] Postgraduate Program in Health Sciences, Federal University of Pelotas, Street Benjamin Constant, 989, Pelotas City 96010-020, Brazil
[2] Postgraduate Program in Health Sciences, Federal University of Rio Grande, Street Visconde De Paranaguá, 102, Rio Grande City 96203-900, Brazil; wlfcfm@gmail.com (W.L.F.C.F.); f.m.r.silvajunior@gmail.com (F.M.R.d.S.J.)
[3] Institute of Biological and Health Sciences, Federal University of Alagoas, Avenue Lourival Melo Mota, S/N, Maceió City 57072-970, Brazil; rodrigo.brum.93@gmail.com
* Correspondence: cienla277@gmail.com

Abstract

Introduction: International studies have demonstrated a positive impact on air quality associated with the presence of green areas in urban conglomerates. However, in Brazil, studies addressing the impacts of urban green areas on air quality are still incipient and are predominantly focused on large urban centers. The objective of this study was to investigate the relationship between urban green areas, surface temperature (LST), and air quality across 15 medium-sized Brazilian cities. Methods: Concentrations of particulate matter fractions (PM_1, $PM_{2.5}$, and PM_{10}) were monitored from January 2023 to May 2024 using second data from low-cost sensors. The NDVI and both daytime and nighttime LST profiles were extracted via Google Earth Engine within a 1 km buffer zone surrounding each station via the Sentinel-2 and MODIS 11A1 satellite data, respectively. Spatial–temporal co-variation patterns were explored using principal component analysis (PCA). To model these dynamics while controlling for spatial dependencies, a multi-criteria framework compared linear models (simple linear regression (LM) and linear mixed (LMM)) and generalized models (generalized additive (GAM) and generalized additive mixed (GAMM)). Results: The results revealed a positive relationship between NDVI and $PM_{2.5}$ and PM_{10} fractions in specific regions, while surface temperatures showed a direct association with finer particles (PM_1 and $PM_{2.5}$). The regression coefficient showed the significant association of PM2.5 with NDVI and nighttime LST ($\beta = 1.330$; IC 95%: [0.397; 2.270]; $p = 0.005$). The GAMM was the best-fitting model for all particle fractions, demonstrating that incorporating monitoring stations as random intercepts successfully controls for unmeasured local heterogeneity, while penalized splines accurately capture non-linear environmental factors. Conclusions: Although many studies have shown that green areas in temperate regions typically act as consistent sinks for particulate matter, our study revealed localized and seasonal responses in tropical urban landscapes. It should be noted that our study is conducted on a national scale and that the use of low-cost sensors and remote sensing does not allow us to distinguish between the localized microclimatic benefits of vegetation and the long-range transport of regional pollutants.

Keywords: air pollutants; urban green areas; low-cost sensors; NDVI; LST

Academic Editor: Kei Sato

Received: 28 April 2026
Revised: 29 May 2026
Accepted: 3 June 2026
Published: 9 June 2026

1. Introduction

Urbanization has significantly contributed to the intensification of air pollution through emissions from industrial activities, the expansion of the vehicle fleet, and other urban dynamics. Studies show that urbanization has contributed to increasing emissions of air pollutants [1,2], increasing temperatures, and the creation of urban heat islands [3]. Air pollution consists of a variable and complex mixture of different substances that can occur in the gaseous, liquid, or solid phase. Among the air pollutants, the following stand out: sulfur dioxide (SO_2), nitrous oxides (NOx), tropospheric ozone (O_3), carbon monoxide (CO), and particulate matter ($PM_{2.5}$, PM_1 and PM_{10}).

The intensification of urbanization, in addition to expanding concrete structures, promotes deforestation, reducing green cover, influencing the increase in pollution levels, and causing impacts on the environment and the health of the urban population [4]. The World Health Organization [5] utilizes these specific indicators to assess global air quality, warning that approximately 9 out of 10 people worldwide are systematically exposed to pollutant levels far exceeding safe health standards, culminating in an estimated 8 million annual premature deaths. Among these monitored pollutants, particulate matter has a robust, evidence-backed causal relationship with cardiovascular anomalies, severe respiratory diseases, and lung cancer [5]. Consequently, air pollution has emerged as one of the most critical urban environmental crises, requiring urgent public interventions to safeguard human health and well-being [6].

An aspect to be considered in urban ecosystems is the progressive increase in land surface temperature (LST) caused by intense building densification and industrialization. The expansion of concrete, asphalt, and low-albedo structures, coupled with horizontal deforestation, drastically reduces urban green cover, alters localized microclimates, and influences ambient pollution levels [4]. These anthropized environments favor the formation of urban heat islands [3] and thermal inversion [7] due to the increase in land surface temperature, promoting the retention of suspended particles in the air. This scenario, along with episodes of wildfires, can aggravate the severity of air quality and cause episodes of acute exposure to the local population and consequently damage to their health.

Even in areas with high green density, forest fires can contribute to the increase in atmospheric substances due to forest fires, mainly $PM_{2.5}$. During forest fire episodes, a small number of particles are produced, among them fine particulate matter ($PM_{2.5}$) [8], and various greenhouse gases, aerosols, and smoke are released into the atmosphere [9]. Most epidemiological and atmospheric studies addressing the relationships between vegetation and air quality remain heavily biased towards megacities in temperate climates, leaving small and medium-sized tropical urban centers structurally underrepresented.

In Brazilian territory, a counterintuitive positive association between NDVI and particulate matter (PM) concentrations can be expected under specific spatiotemporal configurations. Unlike temperate regions, where high NDVI is consistently aligned with pollution mitigation through dry deposition, parts of Brazil (particularly the Amazonian and Central-Western borders) experience intense overlap, where high forest cover temporally coexists with peak regional emissions from biomass burning and long-range transport from agricultural fires during the dry season [10,11]. Brazil had approximately 7% of the world's active forest fires between 2012 and 2017 [12]. The Northern Region of Brazil is one of the main regions that suffer from forest fires due to episodes of drought. Droughts are becoming more frequent throughout the world because of climate change [13]. Therefore, forest fires, due to their magnitude and increased frequency, are a global concern [14], since the dispersion of smoke can reach various areas at considerable distances. The wildfire events in the Northern and Central-Western regions of Brazil in 2024 had national dimensions [15], showing that the impacts of fires can reach areas far from their origin.

Based on these premises, our central hypothesis is that the relationship between urban surface indicators and air quality in medium-sized Brazilian cities is fundamentally non-linear and specific to each season, where the dynamics of forest fires temporarily overlap with localized vegetative mitigation sinks. Therefore, the objective of this study was to explicitly investigate the impact of urban green spaces and land surface temperatures on PM_1, $PM_{2.5}$, and PM_{10} concentrations in 15 medium-sized Brazilian cities using a low-cost integrated sensor network (https://aqicn.org/map/world/), acessed on 7 August 2024 and remote sensing images.

2. Methods

2.1. Study Area

The study area comprises 15 medium-sized municipalities in Brazil (100,000 to 300,000 inhabitants) (Figure 1). These municipalities host at least one air quality monitoring station with a low-cost sensor, covering all five regions of Brazil (North, Northeast, Central-West, Southeast, and South). These sensors are produced in Beijing, China by the Beijing Air Quality project. The distribution of the municipalities and their respective low-cost sensors in each region are listed below.

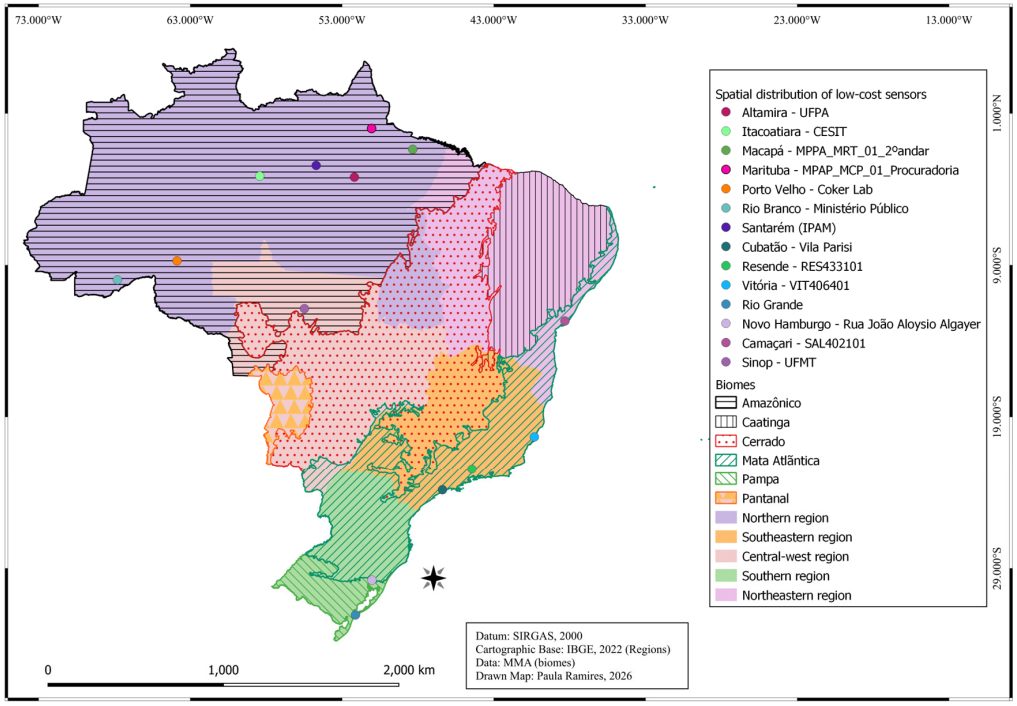

Figure 1. Spatial distribution of low-cost sensors, Brazilian biomes, and regions of Brazil.

2.1.1. Northern Region of Brazil

Municipalities and their respective low-cost sensors (air quality monitoring stations) are as follows: Rio Branco (Rio Branco–Ministério Público and AcreBioClima–UFAC), Altamira (Altamira–UFPA), Itacoatiara (Itacoatiara–CESIT), Macapá (Macapá–MPAP_MCP_01_procuradoria), Marituba (Marituba–MPPA_MRT_01_2º andar), Porto Velho (Porto Velho–Coker Lab), and Santarém (Santarém–IPAM) (Figure 2). The municipalities of Altamira, Itacoatiara, Macapá, Marituba, Porto Velho, Santarém, and Rio Branco are located in the Northern Region of Brazil, characterized by the Amazon biome (dense, large-scale forest), a hot and humid (equatorial) climate, an extensive hydrographic network, and high precipitation levels [16].

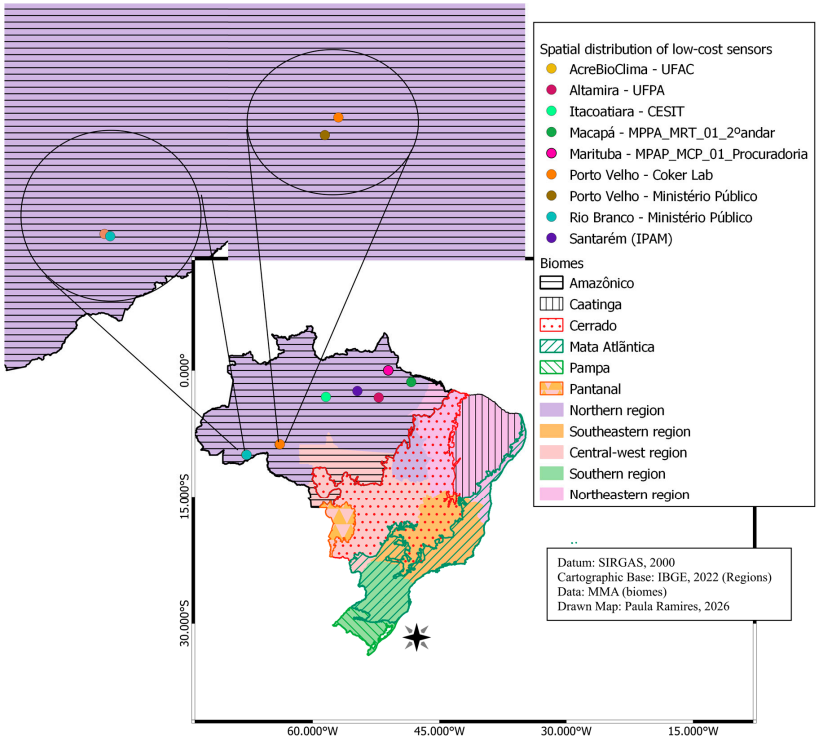

Figure 2. Spatial distribution of low-cost sensors in the Northern Region of Brazil, Brazilian biomes, and regions of Brazil.

2.1.2. Northeastern Region of Brazil

The municipality and its respective low-cost sensor (air quality monitoring station): Camaçari (Camaçari–SAL402101) (Figure 3). The Northeastern Region is characterized by the Caatinga, Cerrado, and Atlantic Forest biomes [16]. Camaçari is located within the Atlantic Forest biome, which is characterized by forest vegetation and a humid tropical climate, with higher precipitation during summer and a dry season occurring in winter [16].

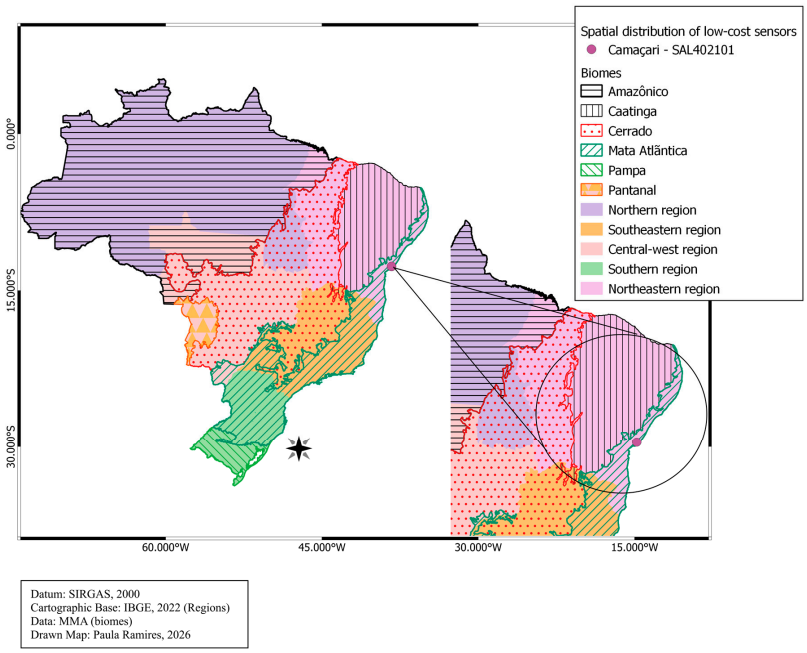

Figure 3. Spatial distribution of low-cost sensors in the Northeastern Region of Brazil, Brazilian biomes, and regions of Brazil.

2.1.3. Central-West Region of Brazil

Municipality and its respective low-cost sensor (air quality monitoring station): Sinop (Sinop–UFMT) (Figure 4). The Central-West Region is influenced by the Cerrado, Amazon, and Pantanal biomes. In the case of Sinop, the predominant biome is the Amazon [16]. In this region, the Amazon biome is characterized by a tropical climate and dense, large-scale forests. However, deforestation for monoculture agriculture has been observed, which has influenced precipitation patterns, leading to longer dry periods (extended dry seasons).

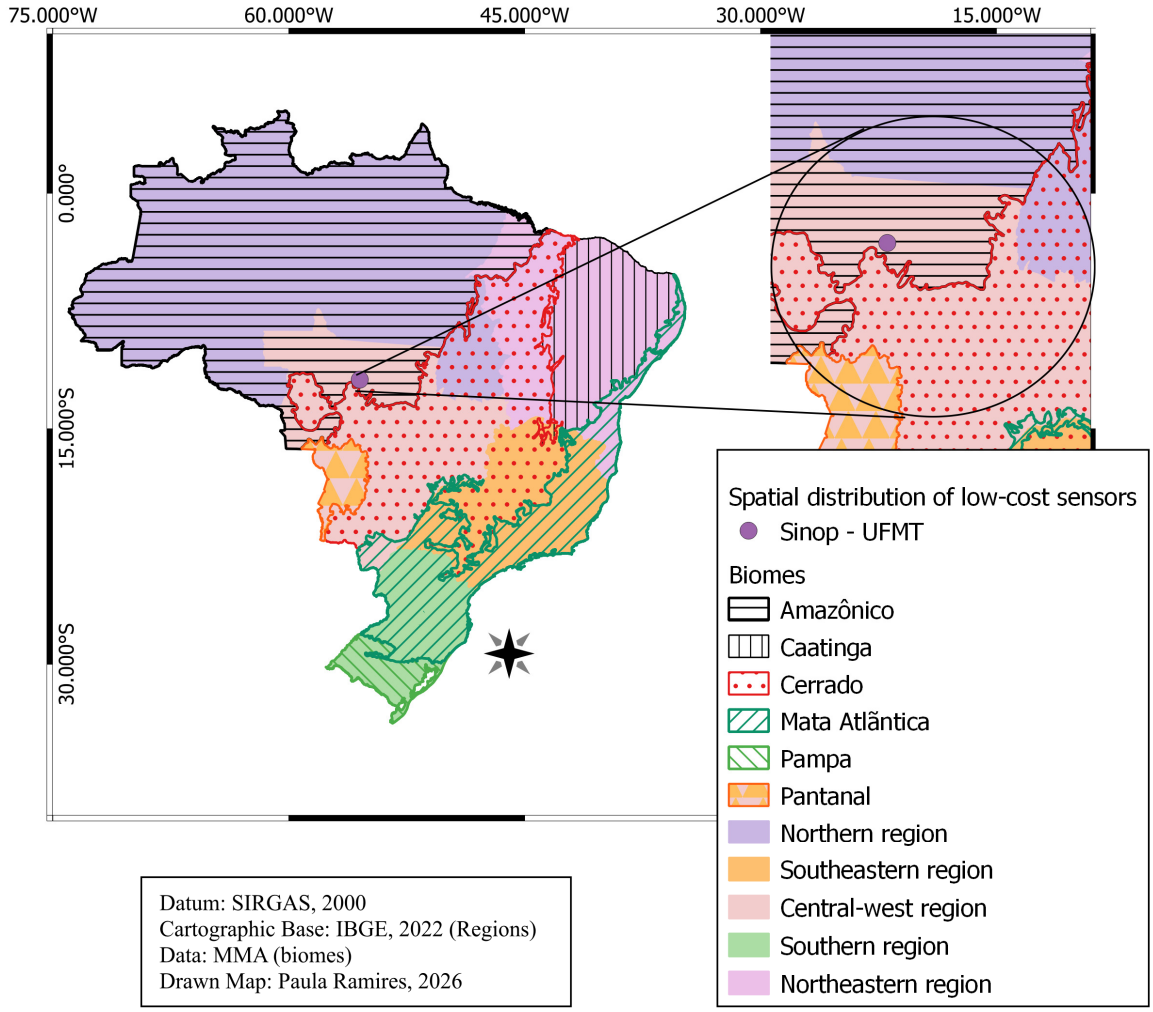

Figure 4. Spatial distribution of low-cost sensors in the Central-West Region of Brazil, Brazilian biomes, and regions of Brazil.

2.1.4. Southeastern Region of Brazil

Municipalities and their respective low-cost sensors (air quality monitoring stations): Cubatão (Cubatão–Centro, Cubatão–CUB400101, Cubatão–Vale de Mogi, Cubatão–Vila Parisi), Resende (RES433101), and Vitória (Vitória–Carapina and Vitória–VIT406401) (Figure 5). This region is predominantly characterized by the Atlantic Forest biome [16]. However, due to intense urbanization and industrialization, significant deforestation of forest vegetation has occurred [17], leaving only remnant areas of the Atlantic Forest.

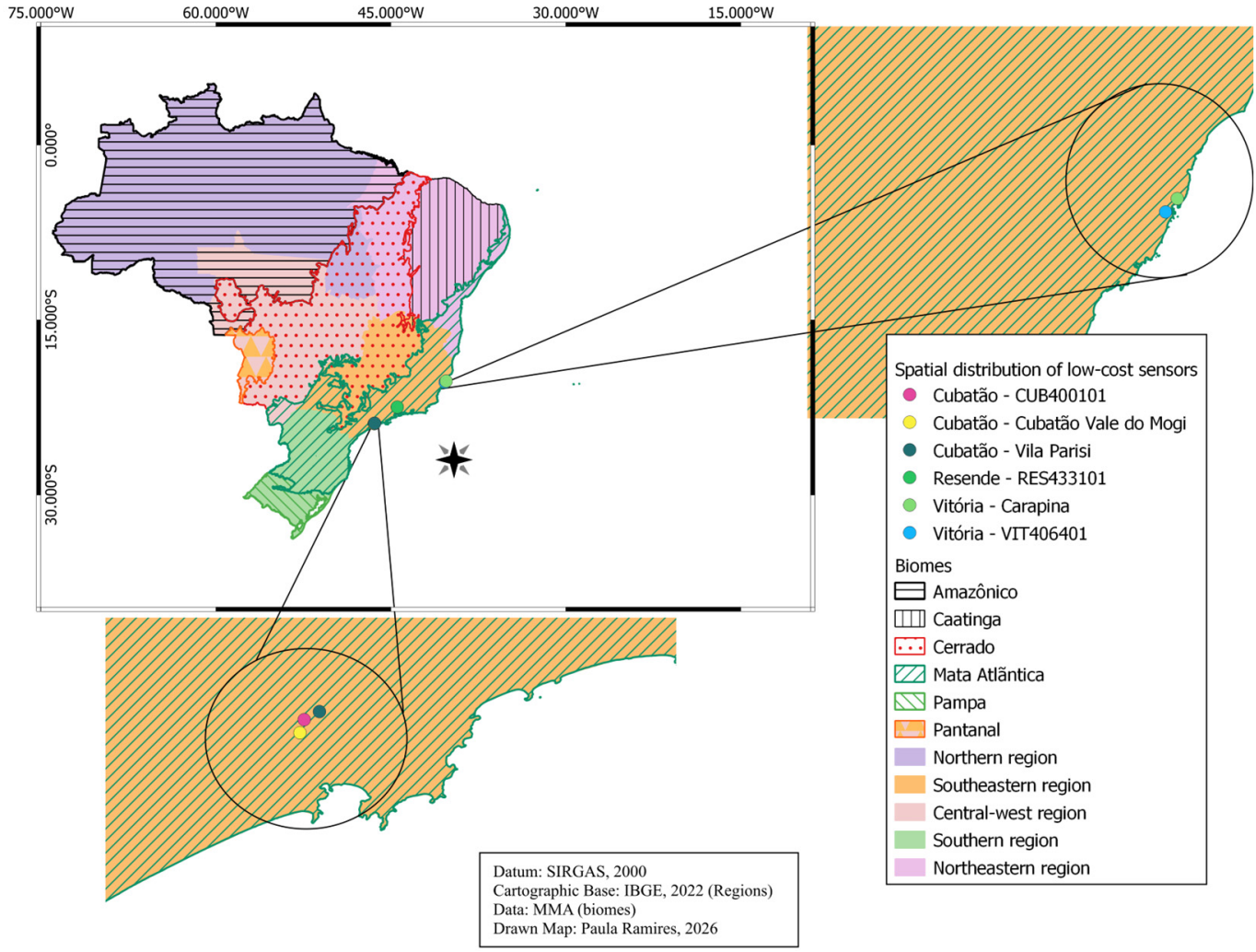

Figure 5. Spatial distribution of low-cost sensors in the Southeastern Region of Brazil, Brazilian biomes, and regions of Brazil.

2.1.5. Southern Region of Brazil

Municipalities and their respective low-cost sensors (air quality monitoring stations): Novo Hamburgo (Novo Hamburgo–Rua João Aloysio Algayer), Rio Grande (Rio Grande), and São Leopoldo (São Leopoldo–Rua América) (Figure 6). These municipalities are located within the Pampa biome, which is characterized by subtropical grasslands with gently rolling hills (coxilhas), mixed prairies, a super-humid subtropical climate, well-distributed precipitation throughout the year, and well-defined seasons, with cold winters and hot summers [16].

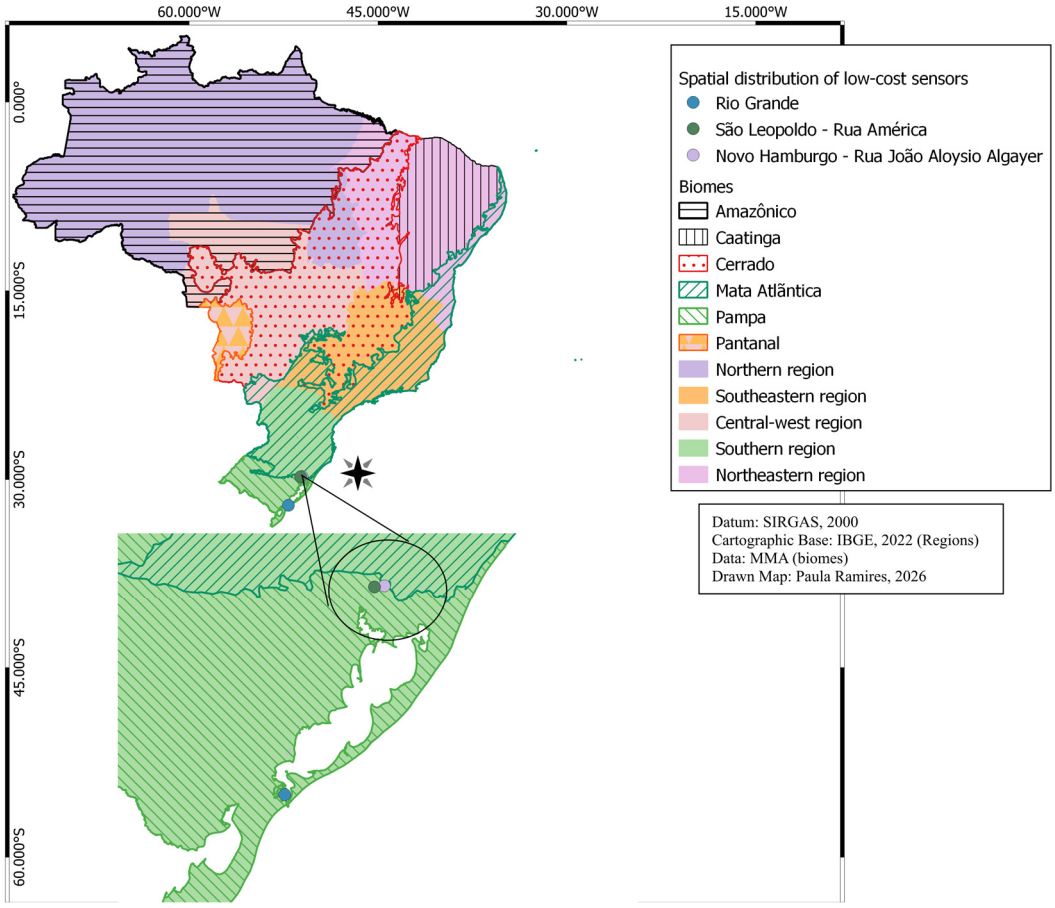

Figure 6. Spatial distribution of low-cost sensors in the Southern Region of Brazil, Brazilian biomes, and regions of Brazil.

2.2. Data Collection

Time series data for particulate matter fractions (PM_1, $PM_{2.5}$, and PM_{10}) were collected in 15 medium-sized Brazilian cities between January 2023 and May 2024. The datasets originate from the GAIA air quality monitoring network, a global citizen science and institutional initiative managed by the World Air Quality Index (WAQI) project, which uses low-cost standardized sensors. The data are published in real time on the internet (https://aqicn.org/map/world/) acessed on 7 August 2024. The datasets were systematically aggregated and processed to calculate monthly average concentrations for subsequent statistical analyses.

The Normalized Difference Vegetation Index (NDVI) was extracted from Sentinel-2 imagery via Google Earth Engine (GEE) between 2023 and 2024, capturing vegetation density within a 1 km radius buffer centered on the geographical coordinates of each air quality monitoring station. For the same temporal window, diurnal and nocturnal Land Surface Temperatures (LST) were retrieved from the MODIS MOD11A1 daily product using GEE. The satellite observations from both sensors were systematically processed to calculate monthly mean values for subsequent statistical analysis.

The 1 km buffer zone was established based on the consolidated literature on micrometeorology and urban climate, which identifies this radius as the microclimatic influence zone determining surface characteristics [18]. In urban land cover studies, land cover characteristics within a 1–2 km radius predominantly shape the local thermal environment (LST) and regulate fine particle deposition patterns [19]. Furthermore, this distance directly corresponds to the nominal spatial resolution (1 km) of the MODIS MOD11A1 daily prod-

uct [20]. Therefore, this radius captures the immediate influence of vegetation density and the influence of the LST on air quality monitoring stations.

2.3. Statistical Analysis

Descriptive statistics, including mean and standard deviation, were initially calculated to characterize the particulate matter datasets (PM_1, $PM_{2.5}$ and PM_{10}). Non-parametric associations were assessed using Spearman's correlation. The regression coefficient was assessed and PCA was also performed. To determine the most robust predictive structure, a multi-criteria modeling framework was deployed, comparing four distinct statistical architectures: linear models (LMs), linear mixed models (LMMs), generalized additive models (GAMs), and generalized additive mixed models (GAMMs). Within the advanced GAMM structure, the non-linear effects of the continuous predictors (NDVI and LST fractions) were modeled using non-parametric penalized cubic regression splines (cr), which were estimated via restricted maximum likelihood (REML) using the mgcv package. The air quality monitoring stations were incorporated into the model as random intercepts using a random-effect penalty basis (s(Station, bs = re)), capturing the baseline variation in particulate matter levels among the different cities.

Temporal autocorrelation was not explicitly analyzed because the data were aggregated monthly, minimizing residual temporal dependence. Model selection and goodness of fit were assessed using the Akaike Information Criterion (AIC), along with the Bayesian Information Criterion (BIC) and adjusted R-squared (R^2adj), to avoid overfitting. All statistical analyses and model estimates were executed in RStudio software Version 4.4.3 (2025-02-28 ucrt). Linear models (LM) were fitted using the base stats package. Linear mixed models (LMMs) were built via the nlme package. The generalized additive models (GAMs) and generalized additive mixed models (GAMMs) were implemented using the mgcv package.

Gaps in the dataset between 2023 and 2024 resulted in overall missing data rates of 19.12% for PM_{10}, 27.06% for PM_{25}, 51.47% for PM_1, 6.76% for daytime LST, and 10.59% for nighttime LST. Gaps in particulate matter data reflected operational maintenance at specific monitoring locations, while the lack of LST data was minimal and driven by localized cloud contamination. These gaps led to an unbalanced panel dataset. To address this, linear mixed models (LMMs) and generalized additive mixed models (GAMMs) were implemented using maximum likelihood estimation routines that handle missing observations by excluding cases with missing data. Including monitoring stations as random intercepts ensures that the variable number of valid temporal entries per location does not bias the fixed-effects regression coefficients (β) or their respective 95% confidence intervals.

3. Results

Air pollutant concentrations varied among air quality monitoring stations, with PM_{10} exhibiting the highest concentrations (Figure 7 and Table S1). In addition, differences were observed in the distribution of particulate matter (PM) concentrations over the study period. NDVI and LST (daytime and nighttime) values (Table 1) indicate that the areas surrounding the central points of the air quality monitoring stations in Itacoatiara–CESIT (0.723) and Novo Hamburgo–Rua João Aloysio Algayer (0.732 in 2024) presented higher levels of vegetation cover. Regarding mean daytime LST, the highest values were recorded in Rio Branco (36.079 °C in 2023 and 34.793 °C in 2024), while the lowest were observed in Rio Grande (21.366 °C in 2023 and 20.307 °C in 2024). The lowest nighttime temperature was also recorded in Rio Grande (14.998 °C in 2024). These factors influenced the concentration levels of particulate matter.

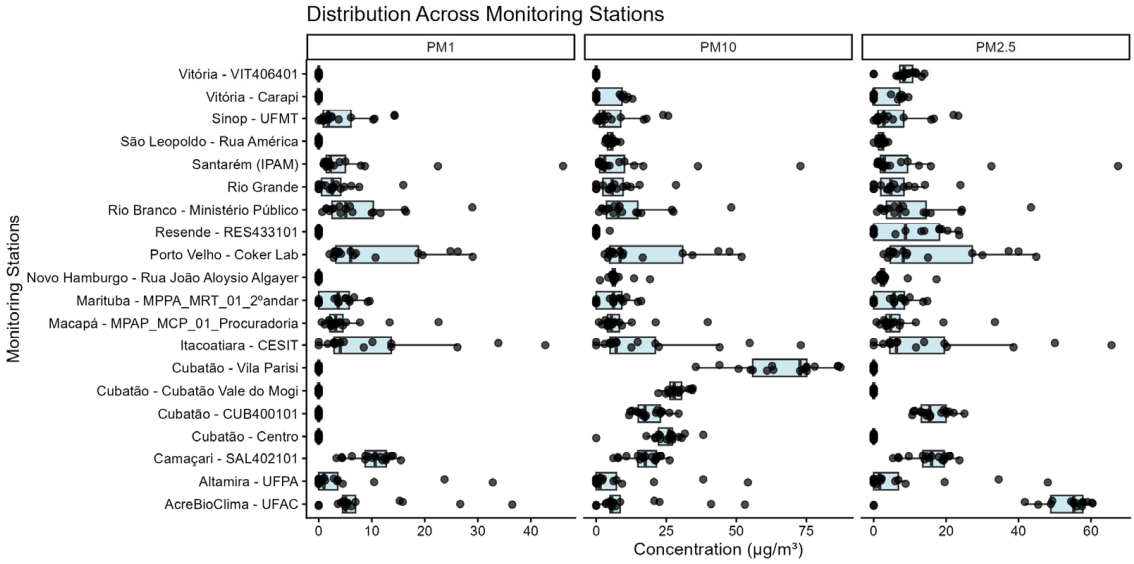

Figure 7. Spatial distribution of monthly particulate matter concentrations (PM_1, $PM_{2.5}$ and PM_{10} ($\mu g/m^3$)) across the monitoring stations in medium-sized Brazilian cities (2023–2024). The black circles represent the mean monthly concentration for each particulate matter fraction (PM_1, $PM_{2.5}$ and PM_{10}), superimposed on the box plots to display the complete data distribution, density, and extreme outlier events at the air quality monitoring stations.

When analyzing Spearman correlations (Figure 8), a strong correlation was observed between PM_1 and $PM_{2.5}$, whereas their correlations with PM_{10} were weaker. A positive, though weak, correlation was found between NDVI and $PM_{2.5}$ and PM_{10} concentrations, while no correlation was observed for PM_1. Regarding land surface temperature (LST), positive correlations were identified with PM_1 and $PM_{2.5}$. The regression coefficient results (Figure 9) demonstrated the effects of NDVI and land surface temperature (daytime and nighttime) on particulate matter. $PM_{2.5}$ showed a significant association with nighttime LST (β = 1.330; IC 95%: [0.397; 2.270]; p = 0.005).

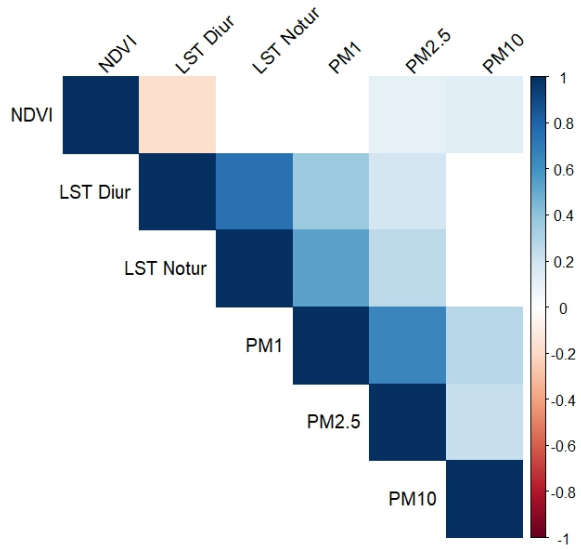

Figure 8. Spearman correlation between PMs (PM1, PM2.5 and PM10), NDVI, and daytime and nighttime land surface temperature (LST).

Table 1. Mean NDVI values (SD) and mean daytime and nighttime LST and their respective SD at air quality monitoring Stations in 2023 and 2024.

	2023						2024					
Air Quality Monitoring Station	*** Mean NDVI**	**SD**	*** Mean Daytime LST**	**SD**	*** Mean Nigthttime LST**	**SD**	*** Mean NDVI**	**SD**	*** Mean Daytime LST**	**SD**	*** Mean Nigtht-time LST**	**SD**
Porto Velho—Ministério Público	0.301	0.031	32.134	2.284	25.891	1.299	0.294	0.029	30.739	2.347	25.528	1.101
Porto Velho—Coker Lab	0.669	0.050	31.902	2.100	23.789	1.639	0.600	0.102	30.667	1.970	24.028	1.218
AcreBioClima—UFAC	0.473	0.074	33.530	2.581	24.316	1.334	0.482	0.116	32.110	2.220	24.080	1.767
Rio Branco—Ministério Público	0.335	0.065	36.079	2.663	24.538	1.628	0.375	0.066	34.793	2.220	24.905	1.251
Itacoatiara—CESIT	0.723	0.112	29.382	2.414	23.684	1.471	0.707	0.099	30.288	1.222	24.280	0.669
Altamira—UFPA	0.458	0.221	29.399	2.144	24.315	0.790	0.500	0.170	29.797	1.670	24.619	0.439
Santarém (IPAM)	0.328	0.056	34.179	2.695	26.313	1.774	0.283	0.043	33.534	2.466	26.518	0.947
Marituba-MPPA_MRT_01_13º andar	0.481	0.102	32.560	2.081	24.447	0.574	0.494	0.071	32.959	1.474	24.487	0.838
Macapá-MPAP_MCP_01_Procuradoria	0.333	0.038	34.705	1.580	25.150	1.226	0.336	0.053	33.285	1.074	25.227	0.592
Camaçari—SAL402101	0.526	0.085	29.749	2.711	22.749	1.773	0.508	0.107	29.958	2.880	23.188	1.829
Vitória—VIT406401	0.381	0.099	28.899	3.342	21.010	1.880	0.277	0.072	29.409	3.046	22.007	1.816
Vitória—Carapina	0.642	0.080	29.997	3.598	22.218	2.045	0.674	0.040	30.346	2.610	23.031	1.365
Resende—RES433101	0.418	0.041	29.404	4.577	18.953	2.972	0.405	0.055	28.760	3.544	19.742	2.745
Cubatão—CUB400101	0.680	0.061	27.354	3.194	19.879	1.668	0.683	0.040	26.848	2.893	20.774	2.522
Cubatão—Cubatão Vale do Mogi	0.421	0.037	29.299	3.916	20.211	1.804	0.436	0.036	27.881	3.049	20.792	1.791
Cubatão—Vila Parisi	0.422	0.055	28.049	3.109	20.121	1.533	0.458	0.056	27.170	2.840	20.228	1.862
Novo Hamburgo—Rua João Aloysio Algayer	0.723	0.022	24.811	4.911	16.212	3.328	0.732	0.023	23.845	6.257	16.376	3.533
Rio Grande	0.312	0.034	21.366	5.860	15.873	4.114	0.324	0.102	20.307	6.648	14.998	4.550
São Leopoldo—Rua América	0.454	0.018	27.400	6.660	17.720	3.766	0.463	0.023	26.575	7.598	17.987	4.242
Sinop—UFMT	0.440	0.147	35.884	3.076	22.758	1.749	0.417	0.128	34.646	1.600	22.630	1.310

* The NDVI, daytime LST, and nighttime LST means are annual.

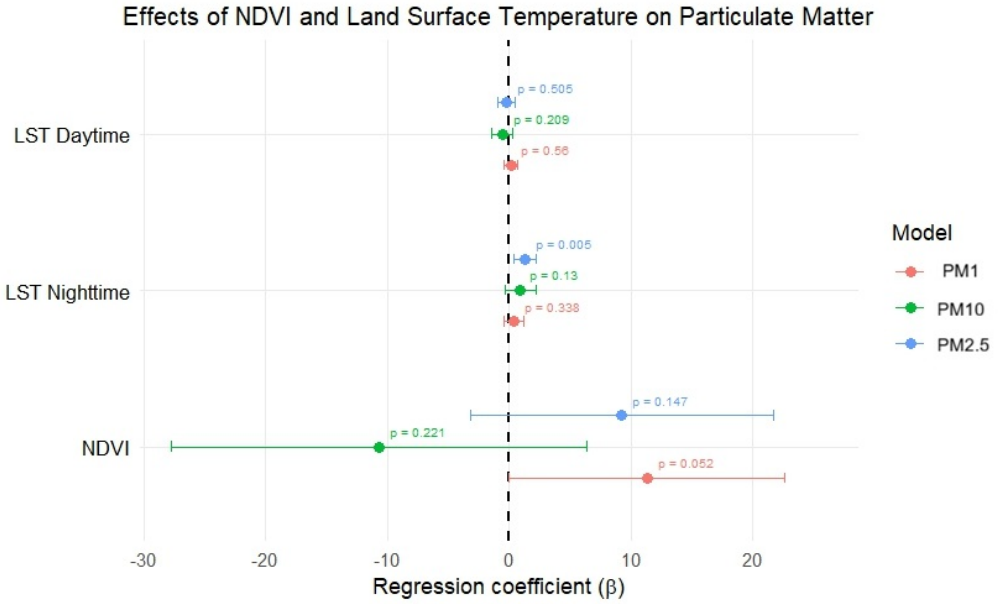

Figure 9. Effect of NDVI and daytime and nighttime land surface temperature (LST) on particulate matter (PMs (PM_1, $PM_{2.5}$ and PM_{10}))—regression coefficient. *p*-values ≤ 0.05 are not significant and *p*-values < 0.01 are significant.

The PCA (Figures 10 and 11) showed that components PC1, PC2, and PC3 explained 81% of the total data variance. PC1 revealed an association between particulate matter concentrations (PM_1, $PM_{2.5}$, and PM_{10}), with this association being stronger between PM_1 and $PM_{2.5}$ is strong. PC1 indicated that air pollution exhibited a higher gradient in stations located in the Northern Region of Brazil—Santarém–IPAM (PC1 = 7.253), Itacoatiara–CESIT (PC1 = 6.218), and AcreBioClima–UFAC (PC1 = 5.215)—although these areas also showed dense vegetation, with PC2 values of 2.964, 4.241, and 2.018, respectively. PC3 showed an association. In these stations, the air contained a higher proportion of coarse particles (PM_{10}) (Santarém–IPAM PC3 = 1.938, Itacoatiara–CESIT PC3 = 0.051, and AcreBioClima–UFAC PC3 = 1.018). In contrast, the stations with lower air pollution gradients were Rio Grande (PC1 = −3.855) and Novo Hamburgo–Rua João Aloysio Algayer (PC1 = −3.092), with PC2 values of 2.311 and 2.235, and PC3 values of 1.704 and −1.294, respectively. The Vitória station (VIT406401) showed that the association between land surface temperature (daytime and nighttime) influences particulate matter concentrations, with PC1 and PC2 values of 0.309 and −2.048, respectively (Table S2).

Air quality monitoring stations exhibited distinct clustering patterns, reflecting spatial differences in environmental conditions. This was confirmed by the model comparison analysis (LM, LMM, GAM, and GAMM) using AIC, in which the GAMM best represented the relationship between particulate matter (PM), NDVI, and land surface temperature (LST; daytime and nighttime). The GAMM showed the lowest AIC values (PM_1 = 870.27, r^2 = 0.375, $PM_{2.5}$ = 1512.95, r^2 = 0.643, PM_{10} = 1793.53, r^2 = 0.705). By employing a GAMM framework, it was possible to capture the spatial heterogeneity between seasons, thus isolating distinct localized environmental dynamics. The model effectively captured seasonal patterns linked to biomass burning in Porto Velho and Rio Branco. Concomitantly, it revealed the pronounced influence of Land Surface Temperature (LST) in coastal urban areas such as Vitória, where elevated surface temperatures likely increase particle resuspension, consequently raising particulate matter concentrations.

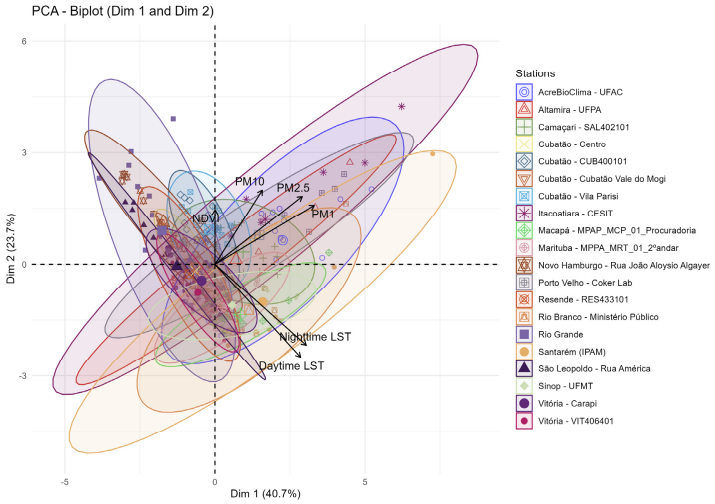

Figure 10. Principal component analysis (PCA) biplot of environmental and air quality variables across the studied monitoring stations (Groups). Vectors indicate the directional influence of particulate matter fractions (PM_1, $PM_{2.5}$, PM_{10}), Normalized Difference Vegetation Index (NDVI), and land surface temperature (daytime and nighttime LST). Individual points and colored 95% confidence ellipses represent the spatiotemporal distribution of data grouped by monitoring station. Dimensions 1 and 2 account for 40.7% and 23.7% of the total variance, respectively. The size of the ellipses indicates the environmental variation and dispersion of data from each air quality monitoring station, where larger ellipses reflect greater variability in the data over the analyzed time period (2023-2024). Longer ellipses show that the air quality monitoring station is influenced by a specific variable. The larger geometric symbols located in the core of each ellipse represent the multivariate average of observations for each station, while the smaller, scattered points represent individual monthly observations.

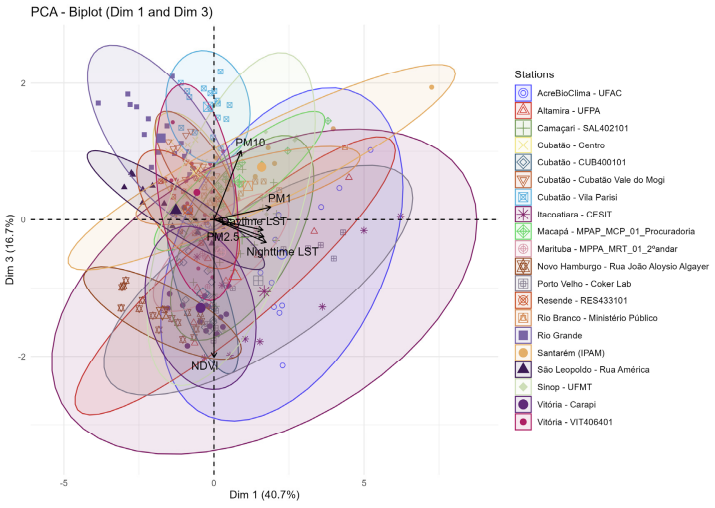

Figure 11. Principal component analysis (PCA) biplot of environmental and air quality variables across the studied monitoring stations (Groups). Vectors indicate the directional influence of particulate matter fractions (PM_1, $PM_{2.5}$, PM_{10}), Normalized Difference Vegetation Index (NDVI), and land surface temperature (daytime and nighttime LST). Individual points and colored 95% confidence ellipses represent the spatiotemporal distribution of data grouped by monitoring station. Dimensions 1 and 3 account for 40.7% and 16.7% of the total variance, respectively. The size of the ellipses indicates the environmental variation and dispersion of data from each air quality monitoring station, where larger ellipses reflect greater variability in the data over the analyzed time period (2023-2024). Longer ellipses show that the air quality monitoring station is influenced by a specific variable. The larger geometric symbols located in the core of each ellipse represent the multivariate average of observations for each station, while the smaller, scattered points represent individual monthly observations.

4. Discussion

The results of the Spearman correlation analyses and the effects of NDVI and land surface temperature (LST; daytime and nighttime) on particulate matter (PM_1, $PM_{2.5}$, and PM_{10}) showed variability in the influence of urban green spaces and LST on PM concentrations across air quality monitoring stations. Furthermore, the findings indicate that higher vegetation density did not necessarily contribute to reductions in PM levels. This may be associated with biomass burning, urbanization, and industrial activities, which promote the resuspension of particles into the atmosphere. Studies demonstrated the impacts of biomass burning on atmospheric pollutant emissions. Refs. [8,9,15] showed that wildfires in the Northern and Central-Western regions of Brazil had nationwide impacts. These burning events may be intensified by prolonged drought periods associated with climate change [13], influencing seasonality (dry season) and altering land surface temperature.

In our findings, daytime temperatures did not directly influence PM variability, whereas nighttime temperatures showed a positive association, indicating that higher surface temperatures favor the accumulation of PM, particularly $PM_{2.5}$. $PM_{2.5}$ exhibited a significant association with nighttime LST (p = 0.001), suggesting that nighttime LST contributes to increased fine particle concentrations in Brazil. Our results also indicate that areas with higher PM concentrations are associated with high biomass availability (high NDVI) and are affected by forest fires, as well as regions with intense urbanization and industrialization. The reduction in vegetation cover in urban areas contributes to the absorption and re-emission of infrared radiation, increasing land surface temperature [21]. We observed that nighttime LST favors increased PM concentrations, which may be related to reduced atmospheric mixing, the formation of thermal inversions, and/or pollutant accumulation near the surface. Thermal inversions reduce the dispersion of dust, smoke, and other atmospheric pollutants [7], consequently increasing pollutant levels [22,23].

The PCA framework revealed a synchronous spatial–temporal co-variation between NDVI and PM concentrations across specific monitoring stations. In the Northern region of Brazil, Santarém–IPAM, Itacoatiara–CESIT, and AcreBioClima–UFAC stations, this pattern reflects regional seasonal dynamics. Intense emissions from biomass burning coincide temporally with high vegetation indices (NDVI). These fires are typically associated with high land surface temperatures and prolonged periods of drought, which characterize the extensive dry seasons in the Amazon region and lead to the critical degradation of air quality. Some studies have indicated that this region tends to experience longer, more intense, and more frequent dry seasons [11,24], which is a deeply concerning issue as it exacerbates chronic air quality crises.

This vulnerability was drastically exacerbated during the 2023–2024 climate anomaly, when a strong El Niño event, coupled with exceptionally high sea surface temperatures in the North Atlantic, triggered an unprecedented drought across the entire basin [25]. This thermal and water stress increases the flammability of the fuel in the forest, in addition to trapping plumes of smoke near the surface, and transforms urban centers into dangerous exposure zones because the concentration of particulate matter exceeds international health standards [26,27].

PCA results identified a strong association between LST and PM fractions. While higher LST values increase the concentration of suspended particles [28] influence localized air quality degradation across inland and equatorial regions, coastal and industrial stations such as Vitória (VIT - 406401), indicating that their local atmospheric dynamics are less driven by land surface temperature anomalies and more influenced by industrial mechanical loading or marine microclimates. Conversely, Rio Grande showed that NDVI contributed to a reduction in PM concentrations. Located in a coastal zone, this municipality benefits from distinct meteorological forcing, where strong maritime winds

promote efficient pollutant dispersion and wet deposition, allowing the local vegetation to act effectively as a physical sink for dry deposition. In the Gulf of Mexico, [29] demonstrated reductions in PM due to wind effects and wet deposition. Therefore, the location of monitoring stations influences air quality. The influence of station location was further confirmed through model comparisons (LM, LMM, GAM, and GAMM).

The GAMM presented the lowest AIC values (PM_1 = 870.27, r^2 = 0.375, $PM_{2.5}$ = 1512.95, r^2 = 0.643, PM_{10} = 1793.53, r^2 = 0.705). The relationship between PM and environmental variables (NDVI and LST) is non-linear, with spatial variability associated with monitoring stations. The GAMM allowed the identification of spatial heterogeneity across stations, showing that they behave differently. For example, Porto Velho, Altamira, and Itacoatiara are located in the Northern Region of Brazil, where frequent biomass burning contributes to increased atmospheric particle concentrations. Official reports and regional fire monitoring data from the National Institute for Space Research (INPE) reveal that the Amazon Biome recorded 32% to 67% of its total burned area during 2023, driven by an extreme El Niño-induced drought. This critical environmental pressure persisted into the following year, with burned area proportions ranging between 26% and 60% from January to May 2024 alone [30].

Cubatão (Vila Parisi) and Vitória, in the Southeastern Region, are highly urbanized and industrialized areas, contributing to increased temperatures and deforestation. However, Vitória did not show increased PM or LST levels, unlike Cubatão (Vila Parisi). Being located in a coastal zone, winds in Vitória may contribute to PM dispersion and temperature regulation. Meteorological conditions and station location play a key role in pollutant dispersion [28]. Previous studies have shown that increases in PM concentrations may be associated with meteorological conditions [31] and emission sources [32], reinforcing the spatial dependence of air quality monitoring stations.

Elevated PM concentrations can cause adverse health effects, particularly among vulnerable populations. The primary impacts are cardiorespiratory [33–35], although other effects may occur depending on PM fraction and concentration levels. A study conducted in China demonstrated the synergistic effect of PM_1 and thermal inversion on reduced birth weight for gestational age [36]. After analyzing age-specific mortality rates from cardiovascular diseases attributable to $PM_{2.5}$ between 1990 and 2021, we identified increases of 91.68% and 78.89%, respectively, with higher mortality among individuals aged 80 years or older [37].

Reducing fine and ultrafine particles can improve air quality and, consequently, public health. In several regions worldwide, studies have demonstrated the benefits of urban green spaces in reducing cardiorespiratory diseases and hospital admissions, particularly in China and the United States. A study in China evaluated the association between $PM_{2.5}$ exposure in residential green spaces and blood lipid levels in hypertensive individuals [38]. In the Chinese population, it was also found that reductions in air pollution levels in green areas were associated with improved lipid profiles [39]. In the United States, ref. [40] observed that short-term exposure to particulate matter ($PM_{2.5}$ and PM_{10}) was associated with fewer hospitalizations in areas with greater green space availability.

Overall, previous studies and our findings indicate that critical air quality scenarios contribute to adverse health outcomes in exposed populations. Our study highlights that the presence of green areas does not necessarily guarantee good air quality. Understanding the complexity of green spaces is essential before implementing mitigation strategies aimed at improving air quality.

5. Limitations

Although this study provides a comprehensive, nationwide assessment of air quality dynamics in underrepresented medium-sized Brazilian cities, some structural and methodological limitations must be acknowledged: First, this study relies on secondary data archived by the GAIA platform. While the network uses a centralized calibration algorithm to convert raw optical counts into mass concentrations, independent, in situ validation with colocation of these low-cost sensors against national reference instruments was not operationally feasible for the authors. Since secondary data always presents missing data, statistical models were used to mitigate these losses.

Second, the spatial characterization was based on a fixed buffer zone of 1 km radius to extract surface indicators (NDVI and LST) around the sensors. Although this threshold aligns with neighborhood-scale landscape processes and respects the nominal resolution of MODIS pixels, it represents an operational compromise. It may not capture microscale urban cover configurations or macroscale regional transport routes operating outside this geometric boundary.

Thirdly, our analytical framework omitted explicit time series of important meteorological covariates, including wind speed and direction, localized precipitation volumes, atmospheric stability indices, and planetary boundary layer height (PBLH). These variables are critical factors for particle dispersal and deposition. While our statistical framework mitigated this omission by using a GAMM—in which random intercepts mathematically capture unmeasured, location-specific microclimatic baselines—the complex interaction between meteorological anomalies and couplings between particulate matter and the surface requires caution in interpretation.

Finally, the study relies on a cross-sectional and correlational design. The statistical associations identified by principal component analysis (PCA) and additive mixed models represent patterns of empirical covariance and spatiotemporal alignment, rather than direct causal mechanisms. Consequently, the observed relationships should be treated as ecological hypotheses. Future research should integrate continuous local meteorological datasets, physicochemical characterization of captured particles, and multiscale vertical boundary layer data to isolate the localized microclimatic benefits of vegetation in relation to pollutant transport on a regional macroscale.

6. Conclusions

This study evaluated the non-linear spatiotemporal dynamics between urban surface indicators (NDVI and LST) and particulate matter fractions (PM_1, $PM_{2.5}$, and PM_{10}) in 15 medium-sized Brazilian cities, using secondary data from the GAIA monitoring network. There is a positive correlation between PM, NDVI, and nighttime LST. Additionally, PM_1 and $PM_{2.5}$ are strongly correlated, suggesting a common source. The effects of NDVI and LST on PM indicate that $PM_{2.5}$ has a significant association, with nighttime LST contributing to critical air quality conditions. The Generalized Additive Mixed Model (GAMM) proved to be the most predictive architecture, successfully controlling for unmeasured spatial heterogeneity through the use of random intercepts. Empirical results revealed distinct regional environmental typologies. Areas such as Santarém, Itacoatiara, and Acre-BioClima, which have high biomass availability, represent critical scenarios due to forest fires that increase atmospheric particle concentrations. Another critical scenario is Cubatão, a densely urbanized and industrialized area, where limited pollutant dispersion and thermal inversion can enhance PM levels. On the other hand, coastal municipalities such as Vitória and Rio Grande can benefit from wind-driven pollutant dispersion and wet deposition, allowing urban vegetation to effectively function as a particulate sink. The location of air quality monitoring stations plays a key role in determining PM concentra-

tion levels, influencing air quality and, consequently, public health outcomes. Therefore, public policies focused on urban greening planning should consider local characteristics to effectively improve air quality and reduce health impacts.

Supplementary Materials: The following supporting information can be downloaded at: https://www.mdpi.com/article/10.3390/atmos17060593/s1, Table S1: Mean concentrations of PM_1, $PM_{2.5}$ and PM_{10} ($\mu g/m^3$) and their distribution throughout the study period, Table S2: Monthly principal component analysis (PC1, PC2, and PC3) values from 2023 to 2024.

Author Contributions: Conceptualization, P.F.R.; Methodology, P.F.R. and W.L.F.C.F.; Software, P.F.R., W.L.F.C.F. and R.d.L.B.; Validation, P.F.R., W.L.F.C.F. and R.d.L.B.; Formal Analysis, P.F.R.; Investigation, P.F.R. and W.L.F.C.F.; Resources, P.F.R.; Data Curation, P.F.R., R.d.L.B., W.L.F.C.F. and F.M.R.d.S.J.; Writing—Original Draft Preparation, P.F.R.; Writing—Review & Editing, P.F.R. and F.M.R.d.S.J.; Visualization, P.F.R.; Supervision, F.M.R.d.S.J.; Project administration, P.F.R.; Funding acquisition, P.F.R. All authors have read and agreed to the published version of the manuscript.

Funding: This study was financed in part by the Coordenação Nacional de Desenvolvimento Científico e Tecnológico—Brazil (CNPq), Grants 151248/2024-9 (PFR).

Institutional Review Board Statement: Not applicable.

Informed Consent Statement: Not applicable.

Data Availability Statement: The raw data supporting the conclusions of this article will be made available by the authors on request.

Acknowledgments: The authors thank the Coordenação Nacional de Desenvolvimento Científico e Tecnológico, CNPq, for the Technological and Industrial Development (WLFCF), and Coordenação de Aperfeiçoamento de Pessoal de Nível Superior, CAPES, for the Doctoral scholarships (RLB). During the preparation of this manuscript/study, the authors used ChatGpt (GPT-5.5; OpenAI) for the purposes of translation of the text. The authors have reviewed and edited the output and take full responsibility for the content of this publication.

Conflicts of Interest: The authors declare no conflicts of interest.

References

1. Yau, Y.Y.; Geeraert, N.; Baker, D.M.; Thibodeau, B. Elucidating sources of atmospheric NOX pollution in a heavily urbanized environment using multiple stable isotopes. *Sci. Total Environ.* **2022**, *832*, 154781. [CrossRef]
2. Pacheco, P.; Mera, E.; Fuentes, V. Intensive Urbanization, Urban Meteorology and Air Pollutants: Effects on the Temperature of a City in a Basin Geography. *Int. J. Environ. Res. Public Health* **2023**, *20*, 3941. [CrossRef]
3. Milesi, C.; Churkina, G. Measuring and monitoring urban impacts on climate change from space. *Remote Sens.* **2020**, *12*, 3494. [CrossRef]
4. Festus, I.A.; Omoboye, I.F.; Andrew, O.B. Urban sprawl: Environmental consequence of rapid urban expansion. *Malays. J. Soc. Sci. Humanit. (MJSSH)* **2020**, *5*, 110–118. [CrossRef]
5. WHO-World Health Organization. WHO Global Air Quality Guidelines: Particulate Matter ($PM_{2.5}$ and PM_{10}), Ozone, Nitrogen Dioxide, Sulfur Dioxide and Carbon Monoxide: Executive Summary. 2021. Available online: https://apps.who.int/iris/bitstream/handle/10665/345334/9789240034433-eng.pdf (accessed on 15 April 2026).
6. Özkök, E.A.; Çobanoğlu, G. Spatial evaluation of air quality by biomonitoring of toxic element accumulation in lichens in urban green areas and nature parks on the Anatolian side of Istanbul. *Environ. Monit. Assess.* **2023**, *195*, 908. [CrossRef]
7. Niedźwiedź, T.; Łupikasza, E.B.; Małarzewski, Ł.; Budzik, T. Surface-based nocturnal air temperature inversions in southern Poland and their influence on PM_{10} and $PM_{2.5}$ concentrations in Upper Silesia. *Theor. Appl. Climatol.* **2021**, *146*, 897–919. [CrossRef]
8. Zhang, Y.; Beggs, P.J.; McGushin, A.; Bambrick, H.; Trueck, S.; Hanigan, I.C.; Morgan, G.G.; Berry, H.L.; Linnenluecke, M.K.; Johnston, F.H.; et al. The 2020 special report of the MJA–Lancet Countdown on health and climate change: Lessons learnt from Australia's "Black Summer". *Med. J. Aust.* **2020**, *213*, 490–492.e10. [CrossRef] [PubMed]
9. Dentener, F.; Kinne, S.; Bond, T.; Boucher, O.; Cofala, J.; Generoso, S.; Ginoux, P.; Gong, S.; Hoelzemann, J.J.; Ito, A.; et al. Emissions of primary aerosol and precursor gases in the years 2000 and 1750 prescribed data-sets for AeroCom. *Atmos. Chem. Phys.* **2006**, *6*, 4321–4344. [CrossRef]

10. Marengo, J.A.; Alves, L.M.; Alvala, R.C.; Cunha, A.P.; Brito, S.; Moraes, O.L.L. Climatic characteristics of the 2010–2016 drought in the semiarid Northeast Brazil region. *Acad. Bras. Cienc.* **2018**, *90*, 1973–1985. [CrossRef] [PubMed]
11. Aragão, L.E.; Anderson, L.O.; Fonseca, M.G.; Rosan, T.M.; Vedovato, L.B.; Wagner, F.H.; Silva, C.V.; Silva Junior, C.H.; Arai, E.; Aguiar, A.P.; et al. 21st-century drought-related fires counteract the Amazon rainforest carbon sink. *Nat. Commun.* **2018**, *9*, 536. [CrossRef] [PubMed]
12. Scott, E. Brazilian forest fires cause toxic air pollution. *Nat. Rev. Earth Environ.* **2023**, *4*, 431. [CrossRef]
13. Masson-Delmotte, V.; Zhai, P.; Pörtner, H.O.; Roberts, D.; Skea, J.; Shukla, P.R.; Pirani, A.; Moufouma-Okia, W.; Péan, C.; Pidcock, R.; et al. Global warming of 1.5 C. *IPCC Spec. Rep. Impacts Glob. Warm.* **2018**, *1*, 43–50.
14. Xu, R.; Yu, P.; Abramson, M.J.; Johnston, F.H.; Samet, J.M.; Bell, M.L.; Haines, A.; Ebi, K.L.; Li, S.; Guo, Y. Wildfires, global climate change, and human health. *N. Engl. J. Med.* **2020**, *383*, 2173–2181. [CrossRef] [PubMed]
15. Tavella, R.A.; de Moura, F.R.; da Silva Júnior, F.M.R. Ashes of governance: Brazil's 2024 wildfire crisis and its implications. *Reg. Environ. Change* **2025**, *25*, 123. [CrossRef]
16. IBGE. *Terrestrial Natural Domains and Regions of Brazilian Biomes: A Proposal for Natural Regionalization [Domínios e Regiões Naturais Terrestres dos Biomas do Brasil: Uma Proposta de Regionalização Natural]*; Brazilian Institute of Geography and Statistics, Coordination of Environment: Rio de Janeiro, Brazil, 2025; p. 233.
17. MapBioma. Available online: https://brasil.mapbiomas.org/dados-do-modulo-mapbiomas-degradacao/ (accessed on 15 April 2026).
18. Oke, T.R.; Mills, G.; Christen, A.; Voogt, J.A. *Urban Climates*; Cambridge University Press: Cambridge, UK, 2017.
19. Estoque, R.C.; Murayama, Y.; Myint, S.W. Effects of landscape composition and pattern on land surface temperature: An urban heat island study in the megacities of Southeast Asia. *Sci. Total Environ.* **2017**, *577*, 349–359. [CrossRef]
20. Wan, Z. New refinements and validation of the collection-6 MODIS land-surface temperature products. *Remote Sens. Environ.* **2014**, *140*, 108–114. [CrossRef]
21. Yadav, N.; Rajendra, K.; Awasthi, A.; Singh, C.; Bhushan, B. Systematic exploration of heat wave impact on mortality and urban heat island: A review from 2000 to 2022. *Urban Clim.* **2023**, *51*, 101622. [CrossRef]
22. Tunno, B.J.; Michanowicz, D.R.; Shmool, J.L.C.; Kinnee, E.; Cambal, L.; Tripathy, S.; Gillooly, S.; Roper, C.; Chubb, L.; E Clougherty, J. Spatial variation in inversion-focused vs 24-h integrated samples of $PM_{2.5}$ and black carbon across Pittsburgh, PA. *J. Expo. Sci. Environ. Epidemiol.* **2016**, *26*, 365–376. [CrossRef]
23. Wallace, J.; Corr, D.; Kanaroglou, P. Topographic and spatial impacts of temperature inversions on air quality using mobile air pollution surveys. *Sci. Total Environ.* **2010**, *408*, 5086–5096. [CrossRef]
24. Marengo, J.A.; Souza, C.M.; Thonicke, K.; Burton, C.; Halladay, K.; Betts, R.A.; Alves, L.M.; Soares, W.R. Changes in climate and land use over the amazon region: Current and future variability and trends. *Front. Earth Sci.* **2018**, *6*, 228. [CrossRef]
25. Jiménez-Muñoz, J.C.; Mattar, C.; Barichivich, J.; Santamaría-Artigas, A.; Takahashi, K.; Malhi, Y.; Sobrino, J.A.; Schrier, G.V.D. Record-breaking warming and extreme drought in the Amazon rainforest during the course of El Niño 2015–2016. *Environ. Res. Lett.* **2024**, *19*, 044002. [CrossRef]
26. Artaxo, P.; Rizzo, L.V.; Brito, J.F.; Barbosa, H.M.J.; Arana, A.; Sena, E.T.; Cirino, G.G.; Bastos, W.; Martine, S.T.; Andreae, M.O. Atmospheric aerosols in Amazonia and land use change: From natural biogenic to biomass burning conditions. *Faraday Discuss.* **2013**, *165*, 203–235. [CrossRef] [PubMed]
27. de Oliveira, G.; Chen, J.M.; Mataveli, G.A.V.; Chaves, M.E.D.; Seixas, H.T.; Cardozo, F.d.S.; Shimabukuro, Y.E.; He, L.; Stark, S.C.; dos Santos, C.A.C. Rapid Recent Deforestation Incursion in a Vulnerable Indigenous Land in the Brazilian Amazon and Fire-Driven Emissions of Fine Particulate Aerosol Pollutants. *Forests* **2020**, *11*, 829. [CrossRef]
28. Islam, A.; Pattnaik, N.; Moula, M.; Rötzer, T.; Pauleit, S.; Rahman, M.A. Impact of urban green spaces on air quality: A study of PM10 reduction across diverse climates. *Sci. Total Environ.* **2024**, *955*, 176770. [CrossRef] [PubMed]
29. Ayala-Cortés, M.; Barrera-Huertas, H.A.; Sedeño-Díaz, J.E.; López-López, E. Impact of particulate matter (PM_{10} and $PM_{2.5}$) from a thermoelectric power plant on morpho-functional traits of *Rhizophora mangle* L. leaves. *Forests* **2023**, *14*, 976. [CrossRef]
30. INPE. GFs/Wildfire Database (BDQueimadas). National Institute for Space Research: São José dos Campos, Brazil. Available online: https://terrabrasilis.dpi.inpe.br/queimadas/portal/pages/secao_relatorio/boletim-infoqueima/index.html (accessed on 25 May 2026).
31. Nguyen, Q.V.; Liou, Y.A. Green space pattern, meteorology, and air pollutants in Taiwan: A multifaceted connection. *Sci. Total Environ.* **2024**, *914*, 169883. [CrossRef]
32. Meleux, F.; Solmon, F.; Giorgi, F. Increase in summer European ozone amounts due to climate change. *Atmos. Environ.* **2007**, *41*, 7577–7587. [CrossRef]
33. Trinh, T.T.; Trinh, T.T.; Le, T.T.; Nguyen, T.D.H.; Tu, B.M. Temperature inversion and air pollution relationship, and its effects on human health in Hanoi City, Vietnam. *Environ. Geochem. Health* **2019**, *41*, 929–937. [CrossRef]

34. Beard, J.D.; Beck, C.; Graham, R.; Packham, S.C.; Traphagan, M.; Giles, R.T.; Morgan, J.G. Winter Temperature Inversions and Emergency Room Visits for Asthma in Salt Lake County, Utah, 2003–2008. *Environ. Health Perspect.* **2012**, *120*, 1385–1390. [CrossRef]
35. Abdul-Wahab, S.A.; Bakheit, C.S.; Siddiqui, R. Study the relationship between the health effects and characterization of thermal inversions in the Sultanate of Oman. *Atmos. Environ.* **2005**, *39*, 5466–5471. [CrossRef]
36. Zhang, X.; Zhang, F.; Gao, Y.; Zhong, Y.; Zhang, Y.; Zhao, G.; Zhu, S.; Zhang, X.; Li, T.; Chen, B.; et al. Synergic effects of PM1 and thermal inversion on the incidence of small for gestational age infants: A weekly-based assessment. *J. Expo. Sci. Environ. Epidemiol.* **2023**, *33*, 652–662. [CrossRef]
37. Zhao, Y.; Yang, X.; Du, Y.; Chen, L.; Dong, J.; Hu, T.; Sun, N.; Sun, Q.; Liang, W.; Wei, X.; et al. Global cardiovascular disease burden attributable to particulate matter pollution, 1990–2021: An analysis of the global burden of disease study 2021 and forecast to 2045. *BMC Cardiovasc. Disord.* **2025**, *25*, 401. [CrossRef] [PubMed]
38. Lei, R.; Zhang, L.; Liu, X.; Liu, C.; Xiao, Y.; Xue, B.; Wang, Z.; Hu, J.; Ren, Z.; Luo, B. Residential greenspace and blood lipids in an essential hypertension population: Mediation through PM2.5 and chemical constituents. *Environ. Res.* **2024**, *240*, 117418. [CrossRef]
39. Wang, Q.; Li, X.; Zhong, W.; Liu, H.; Feng, C.; Song, C.; Yu, B.; Fu, Y.; Lin, X.; Yin, Y.; et al. Residential greenness and dyslipidemia risk: Dose-response relations and mediation through BMI and air pollution. *Environ. Res.* **2023**, *217*, 114810. [CrossRef] [PubMed]
40. Heo, S.; Bell, M.L. The influence of green space on the short-term effects of particulate matter on hospitalization in the US for 2000–2013. *Environ. Res.* **2019**, *174*, 61–68. [CrossRef] [PubMed]